SPANDIDOS PUBLICATIONS

ONCOLOGY LETTERS 11: 4077-4082, 2016

Clinicopathological implications of *GNAS* in Ewing sarcoma

BYEONG-JOO NOH[1], JI-YOUN SUNG[1], YOUN WHA KIM[1], EDUARDO SANTINI ARAUJO[2], RICARDO KARAM KALIL[3], WOON-WON JUNG[4], HYUN-SOOK KIM[5] and YONG-KOO PARK[1]

[1]Department of Pathology, School of Medicine, Kyung Hee University Hospital, Seoul 02447, Republic of Korea; [2]Laboratory of Orthopedic Pathology, Central Army Hospital, Buenos Aires C1426BOR, Argentina; [3]Molecular Pathology Division, SARAH Network of Rehabilitation Hospitals, Brasilia 70335-901, Brazil; [4]Department of Biomedical Laboratory Science, College of Health Science, Korea University, Seoul 02708; [5]Department of Biomedical Laboratory Science, College of Health Sciences, Cheongju University, Chungcheongbuk 28503 Republic of Korea

Received December 12, 2014; Accepted January 19, 2016

DOI: 10.3892/ol.2016.4521

Abstract. The objective of the present study was to determine whether guanine nucleotide-binding protein α stimulating (*GNAS*) gene expression correlates with pathognomonic signs by analyzing the mutations, methylation status and G-protein α subunit ($G_{s\alpha}$) expression of *GNAS* in Ewing sarcoma (ES). Formalin-fixed paraffin-embedded tissue samples from 77 patients with primary ES were obtained in South Korea, Argentina and Brazil, and were studied via methylation chip assay and direct sequencing of the *GNAS* gene and immunohistochemical analysis of $G_{s\alpha}$. The mutation and methylation statuses of the *GNAS* gene were examined. Immunohistochemical results were measured with respect to proportion and staining intensity. The results revealed that *GNAS* genes in ES tumor samples were less methylated compared with normal controls. No mutations were detected at exons 8 or 9 of the *GNAS* locus complex on chromosome 20q13.3, indicating that the pathogenesis of ES was not associated with *GNAS* mutation. $G_{s\alpha}$ expression correlated well with the methylation status of the *GNAS* gene. Notably, high $G_{s\alpha}$ expression was detected more frequently in samples from living patients than from decedents, although this was not statistically significant (P=0.055). In conclusion, *GNAS* mutation is not associated with the pathogenesis of ES tumors. This finding may be used to differentiate ES tumors from metastatic bone lesions with morphological similarity to ES tumors. Analysis of the methylation status of the *GNAS* gene and immunohistochemical $G_{s\alpha}$ expression suggests that hypermethylated *GNAS* (low $G_{s\alpha}$ expression) in ES may be associated with unfavorable progression with a non-significant trend.

Correspondence to: Professor Yong-Koo Park, Department of Pathology, School of Medicine, Kyung Hee University Hospital, 23 Kyungheedaero, Dongdaemun, Seoul 02447, Republic of Korea
E-mail: ykpark@khmc.or.kr

Key words: GNAS, Ewing sarcoma

Introduction

Ewing sarcoma (ES) is the second most common primary bone malignancy, and typically develops in children and adolescents, predominantly in white males (1). It is also referred to as Ewing sarcoma family tumor (ESFT), which includes extraskeletal ES and primitive neuroectodermal tumors. ESFT is a highly aggressive malignancy, with a rate of metastasis of 27% at the time of diagnosis (1). Chemotherapy with intercalated locoregional managements, such as surgery and radiation, is the generally recommended treatment (2). The advanced development of diagnostic tools and delicate understanding of transcriptional and translational factors associated with the pathogenetic Ewing sarcoma breakpoint region 1 (EWSR1)/Friend leukemia integration 1 transcription factor (FLI1) fusion protein (EWS-FLI1) gene have contributed to the improvement of targeted therapies for important oncoproteins. Therefore, the survival rate of patients suffering from ES tends to increase with better elucidation of the pathogenesis and the application thereof to the development of management strategies; the 5-year survival rate may increase from 15 to 39% for metastatic disease, and from 44 to 68% for localized disease (1). For this reason, it is important to determine and act based upon the pathognomonic signs of ES; however, the pathogenesis of ES remains to be elucidated.

There have been a number of suggestions attempting to explain the complicated pathogenesis of ES, which have included insulin-like growth factor-binding protein 3 down-regulation, sonic hedgehog signaling and microsatellite-related signaling (3). Additionally, there is evidence to suggest that expression of the guanosine nucleotide-binding protein α stimulating (*GNAS*) gene, which encodes the G-protein α subunit ($G_{s\alpha}$), is associated with the pathogenesis of ES: i) Insulin-like growth factor 1 receptor (*IGF1R*) expression is related to the early growth response 1 (*EGR1*) gene and its promoters, which consist of the EWS-FLI1 fusion protein and the cyclic adenosine monophosphate (cAMP) response element-binding protein (CREB) (4-6); this cAMP/CREB signature is activated by $G_{s\alpha}$ and may result in *EGR1* and *IGF1R* expression; ii) it has been shown that CREB-Smad6-Runx2 signaling promotes defective

osteogenesis (7), and the EWS-FLI1 fusion protein also inhibits Runx2 (8); iii) our previous genome-wide methylation studies of ES revealed that the *GNAS* gene was hypomethylated (9), and proposed that a hypomethylated *GNAS* gene may be over-expressed in ES relative to normal mesenchymal cells of bone, such that ES tumors would have high expression of $G_{s\alpha}$; and iv) activating mutations of the *GNAS* gene have been identified in pituitary tumors (10), ovarian granulosa cell tumors (11), renal cell carcinomas (12) and hepatocellular carcinomas (13), and these tumors exhibited morphological resemblances to neuro-endocrine cells, similar to ES. On the basis of this evidence, we hypothesized that *GNAS* expression may be associated with the pathogenesis of ES.

The purposes of the present study were to analyze *GNAS* mutation and methylation statuses, and $G_{s\alpha}$ expression in ES, in order to determine whether *GNAS* expression is pathognomonically relevant. To the best of our knowledge, the current study is the first to examine the pathogenic role of the *GNAS* gene in ES.

Materials and methods

Clinical tumor samples. Formalin-fixed paraffin-embedded (FFPE) tissue samples from 77 patients with primary ES were obtained at the Kyung Hee University Hospital in Korea, Central Army Hospital in Argentina and SARAH Network of Rehabilitation Hospitals in Brazil between January 2000 and December 2005. Normal control samples were obtained from the remaining tissues following total knee replacement surgery due to degenerative osteoarthritis at the Kyung Hee University Hospital in Korea. At the time of tumor sampling, patients had no history of chemotherapy or radiation therapy and there was no evidence of metastatic disease. These tumor samples were diagnosed according to the World Health Organization criteria (14) which, in brief, consist of the following: Small round cell sarcomas, showing diffuse membranous CD99 immunostaining, cytoplasmic periodic acid-Schiff staining, and *EWSR1* gene translocation demonstrated via fluorescence *in situ* hybridization (Zytolight SPEC ROS1 and RET Dual Color Break Apart Probes; ZytoVision, Bremerhaven, Germany). If an *EWSR1* gene translocation is not identified but a tumor has a typical immunophenotype in differential diagnosis which is inconsistent with other small round cell tumors, such as lymphoma or rhabdomyosarcoma, such tumor samples are diagnosed as ES.

Patient demographics are presented in Table I. Full data, including follow-up periods and overall survival, were available for 45 patients. The study protocol was reviewed and approved by the Kyung Hee University Institutional Review Board (Seoul, South Korea).

Bisulfite conversion and methylation chip assay. Bisulfite conversions of all DNA samples were performed using an EZ-96 DNA methylation kit (Zymo Research, Orange, CA, USA) according to the manufacturer's instructions. For each bisulfite conversion, 500 ng of genomic DNA was used. Following bisulfite treatment, quantification of methylcytosine content was conducted using an Illumina GoldenGate Methylation Cancer Panel I microarray (Illumina, Inc., San Diego, CA, USA). The GoldenGate Panel was used to process 1,505 CpG sites from a panel of 807 cancer-related genes. Briefly, bisulfite-converted DNA was allowed to react with biotin and was then hybridized to assay oligos, after which allele-specific extensions and ligations were conducted at 45˚C for 15 min. Ligated products were amplified via polymerase chain reaction (PCR) with the following parameters: 10 min at 37˚C; 34 cycles of 35 sec at 95˚C, 35 sec at 56˚C and 2 min at 72˚C; 10 min at 72˚C; and 5 min at 4˚C. Single-stranded PCR products were prepared by denaturation and hybridized to a Sentrix Array Matrix (GoldenGate Methylation Cancer Panel I). Array hybridization was conducted overnight in a temperature gradient program ranging from 45 to 60˚C, and arrays were imaged using a BeadArray Reader scanner (Illumina, Inc.). Raw methylation ratios were calculated using the Methylation Module in Illumina's BeadStudio following background normalization, which was derived by averaging the signals of a built-in negative control. Each sample was examined in a duplicate manner in the chip assay.

Table I. Demographics of Ewing sarcoma patients (n=77).

Clinicopathological parameter	Value
Age at diagnosis, years	
Range	1-57
Median	17
Gender, n (%)	
Male	45 (58.4)
Female	32 (41.6)
Tumor site, n (%)	
Peripheral	48 (62.3)
Central	29 (37.7)
Follow-up, months	
Range	6-96
Median	30.5
Lung metastasis, n (%)	
Present	6 (7.8)
Absent	39 (50.6)
Not available	32 (41.6)
Patient outcome, n (%)	
Survived	25 (32.5)
Died	20 (26.0)
Not available	32 (41.6)

Direct sequencing. Direct sequencing was performed to detect the mutational status of *GNAS* exons 8 and 9. Genomic DNA was extracted using the Magna Pure LC instrument (Roche Applied Science, Mannheim, Germany). PCR was performed using a thermal cycler (GeneAmp PCR system 9700; Thermo Fisher Scientific, Waltham, MA, USA). PCR ingredients containing 2.5 μl of 10X buffer [50 mM KCl, 10 mM Tris-HCl (pH 8.3), 15 mM $MgCl_2$ and 0.001% gelatin], 2.0 μl of 2.5 mM dNTP, 1.0 μl of forward and reverse primers (10 pmol/μl; Bioneer Corporation, Daejeon, Korea), 0.5 μl of AmpliTaq® DNA Polymerase (5 U/μl; Thermo Fisher Scientific) and 1.0 μl of DNA (50 ng/μl) were mixed with deionized water, at a

Table II. Primer sequences for *GNAS* exons 8 and 9.

GNAS exon	Primer sequence		Amplicon size (bp)
	Forward	Reverse	
8	5'-GTT TCG GTT GGC TTT GGT GA-3'	5'-TGG CTT ACT GGA AGT TGA CT-3'	129
9	5'-GAC ATT CAC CCC AGT CCC TCT-3'	5'-GAA GCA AAG CGT TCT TTA CGA-3'	155

total volume of 25 μl. PCR conditions for amplifying *GNAS* exons 8 and 9 were as follows: Denaturation at 94˚C for 2 min; 40 cycles of denaturation at 94˚C for 30 sec, annealing at 62˚C for 30 sec, and extension at 72˚C for 1 min; and a final extension at 72˚C for 10 min. PCR products were purified for sequencing analysis with the QIAquick PCR purification kit (Qiagen, Valencia, CA, USA). Cycle sequencing was performed with the BigDye® Terminator v3.1 Cycle Sequencing Kit (Thermo Fisher Scientific) according to the manufacturer's protocols, and the reaction mixture was analyzed on an ABI Prism 3100 DNA Sequencer (Applied Biosystem; Thermo Fisher Scientific). Primer sequences for PCR and sequencing are listed in Table II.

Immunohistochemistry. Immunohistochemical stains for anti-G protein α S antibody were performed on FFPE human specimens. Immunohistochemistry procedures were performed on 5 μm tissue sections on a Leica Bond-Max automatic slide stainer (Leica Biosystems Melbourne Pty. Ltd., Melbourne, Australia) using the standard protocol. In brief, the 5 μm sections of FFPE tissues were deparaffinized using Bond Dewax Solution (Cat#. AR9222; Leica Biosystems Newcastle Ltd.), and an antigen retrieval procedure was performed using Proteinase K Solution (ready for use; Cat#. S3020; Dako Korea Co., Ltd., Seoul, Korea) for 7 min at room tempurature. The endogenous peroxidase was quenched by incubation with hydrogen peroxide for 15 min. Sections were incubated for 15 min at ambient temperate with a rabbit monoclonal anti-G protein α S antibody (Cat#. ab83735; Abcam, Cambridge, MA, USA) at a 1:600 dilution. Secondary antibodies goat anti-rabbit biotin-free polymeric horseradish peroxidase and rabbit anti-mouse linker antibody, contained in a Bond Polymer Refine Detection System (Cat#. DS9800; Leica Biosystems Newcastle Ltd., Newcastle, UK), were incubated for 8 min at room temperature. Bound primary antibodies were visualized using DAB with a Bond Polymer Refine Detection System (Cat#. DS9800; Leica Biosystems Newcastle Ltd.) and a Bond-Max automatic slide stainer (Leica Biosystems Melbourne Pty. Ltd.). The nuclei in these sections were counterstained with hematoxylin using a Bond Polymer detection System (Cat#. 9800; Leica Biosystems Newcastle, Ltd.). Pancreatic islet cells, obtained from the remaining tissues of patients that received pancreatectomies due to chronic pancreatitis, were used as a positive external control.

Pathological analysis of immunohistochemistry. The immunohistochemical results were measured and scored with respect to intensity and proportion in positive tumor cells, and were independently reviewed by three pathologists (Drs Byeong-Joo Noh, Ji-Youn Sung and Yong-Koo Park). The staining intensity was graded in a 4-tiered system as follows: No visible brown staining, 0; pale brown, 1+; non-homogeneous brown, 2+; homogeneous dark brown color, 3+. According to the cytoplasmic staining intensity and proportion of positive tumor cells, the final scores of $G_{s\alpha}$ were categorized as grade 0, 1, 2 or 3: Grade 0, absence of $G_{s\alpha}$ staining in 100% of tumor cells; grade 1, intensity 1+ in >70% of tumor cells or intensity 2+ in ≤30% of tumor cells; grade 2, intensity 1+ in >70% of tumor cells, intensity 2+ in >30% but ≤70% of tumor cells or intensity 3+ ≤30% of tumor cells; grade 3, intensity 2+ in >70% of tumor cells or intensity of 3+ in >30% of tumor cells (Fig. 1).

Statistical analysis. Statistical analyses were conducted using SPSS version 12.0 (SPSS, Inc., Chicago, IL, USA). Pearson's χ^2 and independent *t*-tests were conducted to determine correlations between tested values and clinicopathological parameters. Univariate survival analyses were performed to examine the prognostic significance of antibody expression and clinicopathological parameters, according to the Kaplan-Meier curve with a log-rank test. Statistical significance was considered to be indicated by $P<0.05$.

Results

Methylation analysis of the GNAS gene. The degree of methylation of the *GNAS* gene was assessed using the Illumina GoldenGate Methylation Cancer Panel I microarray. The GoldenGate DNA methylation method measures DNA methylation levels as β-values ranging from 0 (no DNA methylation detected) to 1 (complete DNA methylation). The results indicated that the *GNAS* gene in ES tumor samples was less methylated than in normal controls; the mean β-value was 0.48 in ES tumor samples vs. 0.83 in normal control samples, indicating that the *GNAS* gene was overexpressed in ES relative to normal tissue.

Mutation analysis of the GNAS gene. No mutations were detected in exons 8 or 9 of the *GNAS* locus complex on chromosome 20q13.3 in DNA extracted from any of the FFPE tumor samples from the ES patients (Fig. 2), demonstrating that the pathogenesis of ES was not associated with *GNAS* mutation.

Immunohistochemical analysis of $G_{s\alpha}$ expression. The correlation of $G_{s\alpha}$ expression with clinicopathological parameters was analyzed using a binary system approach, grouping low expression (grades 0-1) vs. high expression (grades 2-3). Clinicopathological cases involving missing values or without

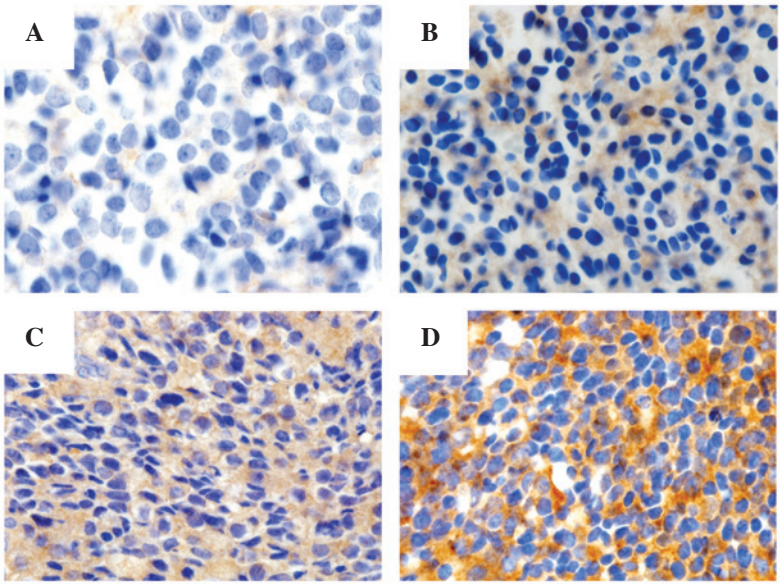

Figure 1. Final immunohistochemical staining cores of G-protein α subunit (visible as brown staining) are classified into 4-tiered system: (A) Grade 0, (B) intensity 1+, (C) intensity 2+ and (D) intensity 3+. Original magnification, x400.

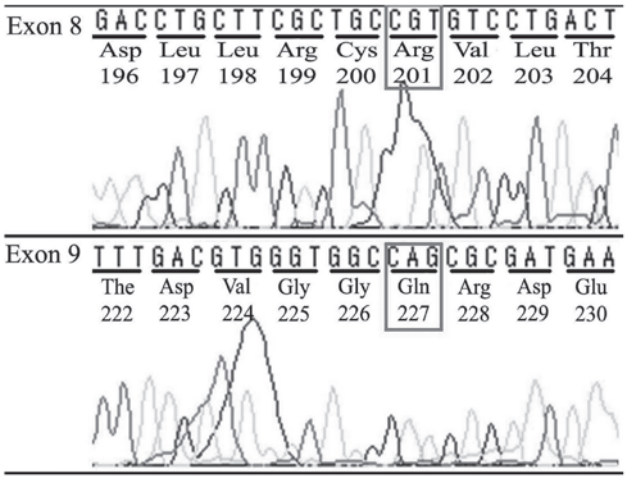

Figure 2. Direct sequencing of *GNAS* exon 8 and 9 detected no mutations, demonstrating that the pathogenesis of Ewing sarcoma was not connected to *GNAS* mutation. *GNAS*, guanine nucleotide-binding protein α stimulating.

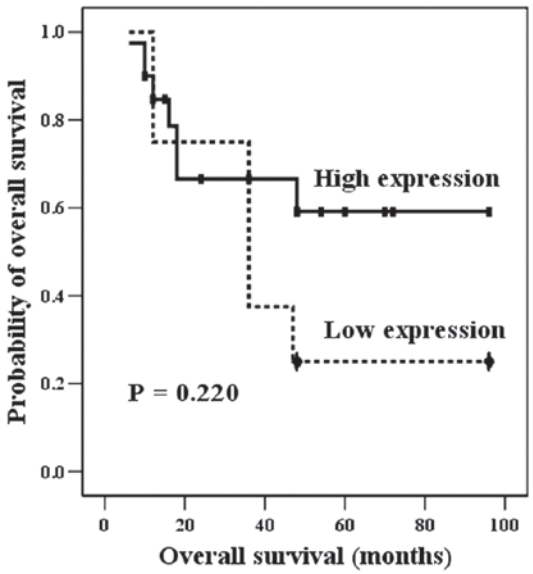

Figure 3. Univariate analysis (Kaplan-Meier curve) demonstrated that high Gsα expression was inclined to indicate more favorable clinical behavior, compared with low Gsα expression, although this was not statistically significant (P=0.220). Gsα, G-protein α subunit.

available clinical information were abbreviated for statistical analyses. Of the 52 ES tumor samples, 34 samples (65.4%) showed high $G_{s\alpha}$ expression, compared with 18 sample (34.6%) with low $G_{s\alpha}$ expression.

$G_{s\alpha}$ expression correlated well with the methylation status of the *GNAS* gene; β-values were 0.681±0.304 in tumor samples with low expression of $G_{s\alpha}$, compared with 0.245±0.229 in samples with high $G_{s\alpha}$ expression (P=0.001) (Table III). High $G_{s\alpha}$ expression in tumor samples was found in 14/17 samples (82.4%) with a hypomethylated *GNAS* gene vs. 1/5 samples (20%) with a hypermethylated *GNAS* gene (P=0.009; Table III).

Notably, high $G_{s\alpha}$ expression was detected more frequently in samples from living patients than decedents, although this was not statistically significant; high $G_{s\alpha}$ was found in 12/15 samples (86.7%) from living patients, vs. 7/13 samples (53.8%) from decedents (P=0.055; Table III). Furthermore, $G_{s\alpha}$ levels were not found to significantly correlate with the survival rate (P=0.220; Fig. 3).

Discussion

The *GNAS* gene on chromosome 20q13.3 encodes the α subunit of the heterotrimeric G protein complex ($G_{s\alpha}$) (15). Activating or inactivating mutations and epigenetic changes at the *GNAS* locus have been described in a variety of human diseases (15).

Activating mutations of the *GNAS* gene induce protein alterations as follows: A mutation at exon 8 of the *GNAS* gene is responsible for substitution of arginine at codon 201 with

Table III. Association of clinicopathological parameters with $G_{s\alpha}$ expression.

Clinicopathological parameter[a]	$G_{s\alpha}$ expression		Total	P-value
	Low	High		
Age, mean ± SD	21.17±11.03	18.62±10.60	19.16 ± 10.50	0.420[b]
Gender, n (%)				0.727[c]
Male	12 (36.4)	21 (63.6)	33 (100.0)	
Female	6 (31.6)	13 (68.4)	19 (100.0)	
Site involved, n (%)				0.451[c]
Peripheral	13 (38.2)	21 (61.8)	34 (100.0)	
Central	5 (27.8)	13 (72.2)	18 (100.0)	
β-value, mean ± SD	0.681±0.304	0.245±0.229	0.478 ± 0.345	0.001[b]
Degree of methylation, n (%)				0.009[c]
Hypomethylation	3 (17.6)	14 (82.4)	17 (100.0)	
Hypermethylation	4 (80.0)	1 (20.0)	5 (100.0)	
Outcome, n (%)				0.055[c]
Survived	2 (13.3)	13 (86.7)	15 (100.0)	
Died	6 (46.2)	7 (53.8)	13 (100.0)	

[a]Clinicopathological cases involving missing values or without available clinicopathological values were removed for statistical analyses; [b]Student's *t*-test; [c]χ^2 test. $G_{s\alpha}$, G-protein α subunit; SD, standard deviation.

cysteine or histidine, termed R201C or R201H, respectively; and, more rarely, a mutation at exon 9 of *GNAS* results in substitution of the glutamine at codon 227 with leucine, arginine, lysine or histidine, termed Q227L, Q227R, Q227K or Q227H, respectively (16). These protein alterations may inhibit GTPase activity, maintaining an active form of $G_{s\alpha}$. Activating mutations of the *GNAS* locus have been detected in McCune-Albright syndrome (17), pituitary adenoma (10), ovarian granulosa cell tumor (11), renal cell carcinoma (12), hepatocellular carcinoma (13), pancreatic intestinal-type intraductal papillary mucinous neoplasm (18,19) and myelodysplastic syndrome (20). As with mesenchymal bone tumors, fibrous dysplasia (2,21) and parosteal osteosarcoma (22) have also been linked to activating mutations of the *GNAS* gene. It has been documented that *GNAS* status has diagnostic utility for differentiating fibro-osseous lesions in morphologically challenging diagnoses: Fibrous dysplasia vs. ossifying fibroma, adamantinoma or osteofibrous dysplasia (16,22,23). *GNAS* mutation was not identified in any ES tumor sample in the current study, indicating that *GNAS* mutation is not associated with the pathogenesis of ES. For this reason, *GNAS* mutation analysis may be used to exclude metastatic bone lesions with *GNAS* mutations, including renal cell carcinoma or hepatocellular carcinoma, which exhibit morphological resemblances to ES tumor cells (24,25).

Inactivating mutations of the *GNAS* locus from the maternal or paternal germ-line are attributed to amino acid substitutions, nonsense mutations, inversions, splicing site mutations, insertions or deletions. Progressive osseous heterotopia has been verified to result from inactivating *GNAS* mutations of predominantly paternal origin (21,26). It has also been documented that epigenetic alterations of the *GNAS* gene are associated with deletion of the syntaxin 16 gene and hypomethylation of the A/B domain at the *GNAS* locus complex (27). Epigenetic changes in the *GNAS* gene have been demonstrated to be important in disease progression in pseudohypoparathyroidism type Ib (28). Until now, there has been no research demonstrating that activating or inactivating mutations or epigenetic changes of *GNAS* have prognostic and not diagnostic value. The T393C pleomorphism of the *GNAS* locus has been identified to have prognostic value in various malignant tumors, including clear cell renal cell carcinoma (29), bladder cancer (30), colorectal cancer (31), epithelial ovarian cancer (32), melanoma (33), glioblastoma (34) and non-small cell lung cancer (35).

In the current study, the epigenetic methylation status of the *GNAS* gene in ES tumor samples was significantly associated with $G_{s\alpha}$ expression: The less methylated *GNAS* gene in ES tumor samples overexpressed $G_{s\alpha}$ (Table III). However, ES patients with hypomethylated *GNAS* genes (high expression of $G_{s\alpha}$) had increased survival probability relative to those with hypermethylated *GNAS* genes (low expression of $G_{s\alpha}$), with a non-significant positive trend (P=0.055, Table III; P=0.220, Fig. 3). On the basis of these results, we speculate that the epigenetic transformation of the *GNAS* gene to hypermethylation status (low $G_{s\alpha}$ expression) in ES tumors may have a an association with more aggressive behavior of ES tumors, but is not significantly correlated with the overall survival.

In summary, *GNAS* mutation is not associated with the pathogenesis of ES tumors. This finding may be used to distinguish metastatic bone lesions with *GNAS* mutations that have morphological similarities to ES tumors. Analysis of the methylation status of the *GNAS* gene and immunohistochemical $G_{s\alpha}$ expression suggests that hypermethylated *GNAS* gene (low $G_{s\alpha}$ expression) in ES may be associated with

unfavorable progression with a non-significant trend. Further studies with a larger sample of patients are required to verify these results.

References

1. Esiashvili N, Goodman M and Marcus RB Jr: Changes in incidence and survival of Ewing sarcoma patients over the past 3 decades: Surveillance epidemiology and end results data. J Pediatr Hematol Oncol 30: 425-430, 2008.
2. Lee SE, Lee EH, Park H, Sung JY, Lee HW, Kang SY, Seo S, Kim BH, Lee H, Seo AN, *et al*: The diagnostic utility of the GNAS mutation in patients with fibrous dysplasia: Meta-analysis of 168 sporadic cases. Hum Pathol 43: 1234-1242, 2012.
3. Lessnick SL and Ladanyi M: Molecular pathogenesis of Ewing sarcoma: New therapeutic and transcriptional targets. Annu Rev Pathol 7: 145-159, 2012.
4. Ma Y, Cheng Q, Ren Z, Xu L, Zhao Y, Sun J, Hu S and Xiao W: Induction of IGF-1R expression by EGR-1 facilitates the growth of prostate cancer cells. Cancer Lett 317: 150-156, 2012.
5. Wu X, Cheng J, Li P, Yang M, Qiu S, Liu P and Du J: Mechano-sensitive transcriptional factor Egr-1 regulates insulin-like growth factor-1 receptor expression and contributes to neointima formation in vein grafts. Arterioscler Thromb Vasc Biol 30: 471-476, 2010.
6. Watson DK, Robinson L, Hodge DR, Kola I, Papas TS and Seth A: FLI1 and EWS-FLI1 function as ternary complex factors and ELK1 and SAP1a function as ternary and quaternary complex factors on the Egr1 promoter serum response elements. Oncogene 14: 213-221, 1997.
7. Fan QM, Yue B, Bian ZY, Xu WT, Tu B, Dai KR, Li G and Tang TT: The CREB-Smad6-Runx2 axis contributes to the impaired osteogenesis potential of bone marrow stromal cells in fibrous dysplasia of bone. J Pathol 228: 45-55, 2012.
8. Li X, McGee-Lawrence ME, Decker M and Westendorf JJ: The Ewing's sarcoma fusion protein, EWS-FLI, binds Runx2 and blocks osteoblast differentiation. J Cell Biochem 111: 933-943, 2010.
9. Park HR, Jung WW, Kim HS and Park YK: Microarray-based DNA methylation study of Ewing's sarcoma of the bone. Oncol Lett 8: 1613-1617, 2014.
10. Gadelha MR, Trivellin G, Hernández, Ramírez LC and Korbonits M: Genetics of pituitary adenomas. Front Horm Res 41: 111-140, 2013.
11. Kalfa N, Ecochard A, Patte C, Duvillard P, Audran F, Pienkowski C, Thibaud E, Brauner R, Lecointre C, Plantaz D, *et al*: Activating mutations of the stimulatory g protein in juvenile ovarian granulosa cell tumors: A new prognostic factor? J Clin Endocrinol Metab 91: 1842-1847, 2006.
12. Kalfa N, Lumbroso S, Boulle N, Guiter J, Soustelle L, Costa P, Chapuis H, Baldet P and Sultan C: Activating mutations of Gsalpha in kidney cancer. J Urol 176: 891-895, 2006.
13. Nault JC, Fabre M, Couchy G, Pilati C, Jeannot E, Tran Van Nhieu J, Saint-Paul MC, De Muret A, Redon MJ, Buffet C, *et al*: GNAS-activating mutations define a rare subgroup of inflammatory liver tumors characterized by STAT3 activation. J Hepatol 56: 184-191, 2012.
14. de alava E, Lessnick SL and Sorensen PH: Ewing sarcoma. In: WHO classification of Tumours of Soft Tissue and Bone. Fletcher CDM, Bridge JA, Hogendoorn PCW and Mertens F (eds). 4th edition. IARC Press, Lyon, pp305-309, 2012.
15. Weinstein LS, Liu J, Sakamoto A, Xie T and Chen M: Minireview: GNAS: Normal and abnormal functions. Endocrinology 145: 5459-5464, 2004.
16. Tabareau-Delalande F, Collin C, Gomez-Brouchet A, Decouvelaere AV, Bouvier C, Larousserie F, Marie B, Delfour C, Aubert S, Rosset P, *et al*: Diagnostic value of investigating GNAS mutations in fibro-osseous lesions: A retrospective study of 91 cases of fibrous dysplasia and 40 other fibro-osseous lesions. Mod Pathol 26: 911-921, 2013.
17. Salpea P and Stratakis CA: Carney complex and McCune Albright syndrome: An overview of clinical manifestations and human molecular genetics. Mol Cell Endocrinol 386: 85-91, 2014.
18. Matthaei H, Wu J, Dal Molin M, Shi C, Perner S, Kristiansen G, Lingohr P, Kalff JC, Wolfgang CL, Kinzler KW, *et al*: GNAS sequencing identifies IPMN-specific mutations in a subgroup of diminutive pancreatic cysts referred to as 'incipient IPMNs'. Am J Surg Pathol 38: 360-363, 2014.
19. Dal Molin M, Matthaei H, Wu J, Blackford A, Debeljak M, Rezaee N, Wolfgang CL, Butturini G, Salvia R, Bassi C, *et al*: Clinicopathological correlates of activating GNAS mutations in intraductal papillary mucinous neoplasm (IPMN) of the pancreas. Ann Surg Oncol 20: 3802-3808, 2013.
20. Bejar R, Stevenson K, Abdel-Wahab O, Galili N, Nilsson B, Garcia-Manero G, Kantarjian H, Raza A, Levine RL, Neuberg D and Ebert BL: Clinical effect of point mutations in myelodysplastic syndromes. N Engl J Med 364: 2496-2506, 2011.
21. Regard JB, Malhotra D, Gvozdenovic-Jeremic J, Josey M, Chen M, Weinstein LS, Lu J, Shore EM, Kaplan FS and Yang Y: Activation of hedgehog signaling by loss of GNAS causes heterotopic ossification. Nat Med 19: 1505-1512, 2013.
22. Carter JM, Inwards CY, Jin L, Evers B, Wenger DE, Oliveira AM and Fritchie KJ: Activating GNAS mutations in parosteal osteosarcoma. Am J Surg Pathol 38: 402-409, 2014.
23. Shi RR, Li XF, Zhang R, Chen Y and Li TJ: GNAS mutational analysis in differentiating fibrous dysplasia and ossifying fibroma of the jaw. Mod Pathol 26: 1023-1031, 2013.
24. Kalfa N, Lumbroso S, Boulle N, Guiter J, Soustelle L, Costa P, Chapuis H, Baldet P and Sultan C: Activating mutations of Gsalpha in kidney cancer. J Urol 176: 891-895, 2006.
25. Nault JC, Fabre M, Couchy G, Pilati C, Jeannot E, Tran Van Nhieu J, Saint-Paul MC, De Muret A, Redon MJ, Buffet C, *et al*: GNAS-activating mutations define a rare subgroup of inflammatory liver tumors characterized by STAT3 activation. J Hepatol 56: 184-191, 2012.
26. Pignolo RJ, Xu M, Russell E, Richardson A, Kaplan J, Billings PC, Kaplan FS and Shore EM: Heterozygous inactivation of Gnas in adipose-derived mesenchymal progenitor cells enhances osteoblast differentiation and promotes heterotopic ossification. J Bone Miner Res 26: 2647-2655, 2011.
27. Turan S, Ignatius J, Moilanen JS, Kuismin O, Stewart H, Mann NP, Linglart A, Bastepe M and Jüppner H: De novo STX16 deletions: An infrequent cause of pseudohypoparathyroidism type Ib that should be excluded in sporadic cases. J Clin Endocrinol Metab 97: E2314-E2319, 2012.
28. Yuno A, Usui T, Yambe Y, Higashi K, Ugi S, Shinoda J, Mashio Y and Shimatsu A: Genetic and epigenetic states of the GNAS complex in pseudohypoparathyroidism type Ib using methylation-specific multiplex ligation-dependent probe amplification assay. Eur J Endocrinol 168: 169-175, 2013.
29. Frey UH, Lümmen G, Jäger T, Jöckel KH, Schmid KW, Rübben H, Müller N, Siffert W and Eisenhardt A: The GNAS1 T393C polymorphism predicts survival in patients with clear cell renal cell carcinoma. Clin Cancer Res 12: 759-763, 2006.
30. Frey UH, Eisenhardt A, Lümmen G, Rübben H, Jöckel KH, Schmid KW and Siffert W: The T393C polymorphism of the G alpha s gene (GNAS1) is a novel prognostic marker in bladder cancer. Cancer Epidemiol Biomarkers Prev 14: 871-877, 2005.
31. Frey UH, Alakus H, Wohlschlaeger J, Schmitz KJ, Winde G, van Calker HG, Jöckel KH, Siffert W and Schmid KW: GNAS1 T393C polymorphism and survival in patients with sporadic colorectal cancer. Clin Cancer Res 11: 5071-5077, 2005.
32. Tominaga E, Tsuda H, Arao T, Nishimura S, Takano M, Kataoka F, Nomura H, Hirasawa A, Aoki D and Nishio K: Amplification of GNAS may be an independent, qualitative and reproducible biomarker to predict progression-free survival in epithelial ovarian cancer. Gynecol Oncol 118: 160-166, 2010.
33. Frey UH, Fritz A, Rotterdam S, Schmid KW, Potthoff A, Altmeyer P, Siffert W and Brockmeyer NH: GNAS1 T393C polymorphism and disease progression in patients with malignant melanoma. Eur J Med Res 15: 422-427, 2010.
34. El Hindy N, Lambertz N, Bachmann HS, Frey UH, Adamzik M, Zhu Y, Sure U, Siffert W and Sandalcioglu IE: Role of the GNAS1 T393C polymorphism in patients with glioblastoma multiforme. J Clin Neurosci 18: 1495-1499, 2011.
35. Xie FJ, Zhao P, Kou JY, Hong W, Fu L, Hu L, Hong D, Su D, Gao Y and Zhang YP: The T393C polymorphism of GNAS1 as a predictor for chemotherapy sensitivity and survival in advanced non-small-cell lung cancer patients treated with gemcitabine plus platinum. Cancer Chemother Pharmacol 69: 1443-1448, 2012.